Optimal Tap Selection of Step-Voltage Regulators in Multi-Phase Distribution Networks

Mohammadhafez Bazrafshan
Nikolaos Gatsis
Department of Electrical and Computer Engineering
The University of Texas at San Antonio
{mohammadhafez.bazrafshan, nikolaos.gatsis}@utsa.edu

Hao Zhu
Department of Electrical and Computer Engineering
The University of Texas at Austin
haozhu@utexas.edu

***Abstract*—An optimal power flow (OPF) problem is formulated that allows for tap selection of various types of step-voltage regulators (SVRs) in multi-phase distribution networks. The goal of the OPF is power-import minimization while satisfying operational constraints. Variables include nodal power injections, nodal voltages, and SVR tap ratios. SVRs are modeled according to their voltage gains and their connecting transmission line parameters. A set of power flow equations that rely on the nodal admittance model of SVRs and explicitly account for the tap ratios are derived. Chordal SDP relaxations of the power flow equations are pursued for non-SVR edges. For each SVR type, novel relaxations are proposed to handle the non-convex primary-to-secondary voltage relationship. Numerical tests on the IEEE 37-bus feeder indicate the success of the proposed formulation in selecting taps of wye, closed-delta, and open-delta SVRs while keeping the incurred cost within 1% of its optimal value.**

***Index Terms*—Distribution networks, optimal power flow, chordal semidefinite relaxation, step-voltage regulators.**

I. Introduction

A fundamental task in distribution systems engineering is to maintain steady-state voltages within acceptable bounds as specified by ANSI standards [1]. A key apparatus to this purpose is the step-voltage regulator (SVR). Traditionally, taps of SVRs are selected based on local voltage measurements from a load center. This process typically ignores global objectives—as achieved by optimal power flow (OPF) formulations.

To this end, a tap selection mechanism for SVRs is presented in this paper within an OPF framework. The goal is to minimize the power import to the distribution network while respecting operational constraints—a beneficial setup for market structures where operation and retail are bundled. The proposed OPF formulation includes accurate models for multi-phase distribution network elements, and additionally, accounts for tap optimization using the newly-developed nodal admittance models of various SVR types [2].

Recent convex relaxations and approximations of the multi-phase power flow equations have well-equipped the distribution sector to tackle the challenging nonconvex OPF problem [3]–[6], albeit without considering SVRs. Multi-phase distribution OPF with wye SVRs is considered in [7] using mixed-integer nonlinear programming, and in [8] and [9] respectively leveraging the full and chordal semidefinite relaxations of the power flow equations. The works in [8] and [9] eliminate the nonlinear relationship between the currents on primary and secondary sides of SVRs by imposing a linear equality constraint on power injection on each side. The nonconvex primary-to-secondary voltage relationship is handled in [8] via a linear bound on the tap ratios assuming individual tap operation, and in [9] via a semidefinite bound assuming equal taps on every phase of the SVR.

Approaches of [7]–[9] focus solely on wye SVRs for which the secondary voltage of each phase can be regulated independently from other phases. In other commonly used SVRs, such as open-delta or closed-delta, phases are coupled. The implication is that input and output power injections are not equal per phase, and the network cannot be decoupled, as in the methodology of [8] and [9].

This work seeks a multi-phase OPF formulation that encompasses accurate models of the three most common SVRs, including the closed- and open-delta, from [2]. The goal is to minimize the amount of power import to the distribution network while satisfying operational constraints. Instead of decoupling the network, based on the newly-developed admittance models of SVRs, a set of power flow equations that explicitly account for the tap ratios are derived. Chordal semidefinite relaxations of the power flows are then leveraged for non-SVR edges while novel relaxations are proposed to handle the nonconvex primary-to-secondary voltage relationship of SVR edges. The resulting formulation is a semidefinite program (SDP). Numerical tests on the IEEE 37-bus feeder indicate the success of the proposed OPF in regulating voltages while keeping the incurred cost within 1% of its optimal value.

This paper is organized as follows. Section II presents the network model. Section III introduces the nonconvex OPF with SVR tap-selection. Tractability via relaxations is pursued in Section IV. Numerical tests of Section V corroborate the practicality of the proposed formulation. The paper concludes in Section VI by discussing its limitations and future work.

II. Network modeling

This section introduces the notations and the models of the distribution network elements in a three-phase setting. The

This material is based upon work supported by the National Science Foundation under Grant No. CCF-1421583, ECCS-1610732, and ECCS-1653706.

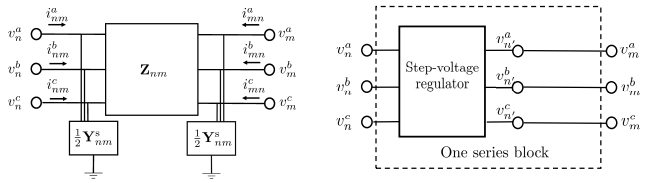

(a) (b)

Figure 1. (a) Three-phase transmission line. (b) Step-voltage regulator in series with a transmission line.

notation $\overline{(.)}$ is used to denote the conjugate transpose of $(.)$.

A. Network and general series element modeling

A multi-phase distribution network is modeled by a directional graph $(\mathcal{N}, \mathcal{E})$, where $\mathcal{N}$ is the set of nodes, and $\mathcal{E} = \{(n,m)\} \subseteq \mathcal{N} \times \mathcal{N}$ is the set of edges. Partition $\mathcal{N}$ as $\mathcal{N} = \mathcal{N}_+ \cup \mathcal{S}$, where, $\mathcal{N}_+$ and $\mathcal{S}$ are respectively the sets of user nodes and slack buses. Partition $\mathcal{E}$ as $\mathcal{E} = \mathcal{E}_{\rm T} \cup \mathcal{E}_{\rm R}$ where $\mathcal{E}_{\rm T}$ collects all edges that represent transmission lines or transformers while $\mathcal{E}_{\rm R}$ collects all edges that represent SVRs.

For a node $n \in \mathcal{N}$ and edge $(n,m) \in \mathcal{E}$, denote respectively their set of available phases by $\Omega_n \subseteq \Omega$ and $\Omega_{nm} \subseteq \Omega$ where $\Omega = \{a,b,c\}$. For the sake of exposition, we assume a three-phase network where $\Omega_n = \Omega_{nm} = \Omega$. A multi-phase setting where some nodes and some edges have missing phases are easily handed using a modeling approach similar to [2].

Let i^ϕ_{nm} and i^ϕ_{mn} respectively denote the current flowing from node n to m and m to n on phase $\phi \in \Omega$ of edge (n,m), and let $\mathbf{i}_{nm} := \{i^\phi_{nm}\}_{\phi\in\Omega}$ and $\mathbf{i}_{mn} := \{i^\phi_{mn}\}_{\phi\in\Omega}$. Figure 1a depicts a transmission line with currents i^ϕ_{nm} and i^ϕ_{mn} marked. Further, denote respectively the voltage and *injected* current phasors at node $n \in \mathcal{N}$ and phase $\phi \in \Omega$ by v^ϕ_n and i^ϕ_n. Collect the voltage and current phasors of node n in $\mathbf{v}_n := \{v^\phi_n\}_{\phi\in\Omega}$ and $\mathbf{i}_n := \{i^\phi_n\}_{\phi\in\Omega}$ and let $\mathbf{v} := \{\mathbf{v}_n\}_{n\in\mathcal{N}}$. Denote the complex power injection at node n and phase ϕ by s^ϕ_n, and let $\mathbf{s}_n := \{s^\phi_n\}_{\phi\in\Omega_n}$ and $\mathbf{s} := \{\mathbf{s}_n\}_{n\in\mathcal{N}}$.

For edge $(n,m) \in \mathcal{E}_{\rm T}$, voltages and currents satisfy

$$\mathbf{i}_{nm} = \mathbf{Y}^{(n)}_{nm}\mathbf{v}_n - \mathbf{Y}^{(m)}_{nm}\mathbf{v}_m,\ (n,m) \in \mathcal{E}_{\rm T} \tag{1a}$$
$$\mathbf{i}_{mn} = \mathbf{Y}^{(m)}_{mn}\mathbf{v}_m - \mathbf{Y}^{(n)}_{mn}\mathbf{v}_n,\ (n,m) \in \mathcal{E}_{\rm T} \tag{1b}$$

where matrices $\mathbf{Y}^{(n)}_{nm}$, $\mathbf{Y}^{(m)}_{nm}$, $\mathbf{Y}^{(m)}_{mn}$, and $\mathbf{Y}^{(n)}_{mn}$ (in $\mathbb{C}^{3\times3}$) for transmission lines are given in [1]. In case of various transformer connections, see e.g. [10].

B. Modeling of SVRs

A three-phase SVR consists of three single-phase autotransformers, typically connected in wye, closed-delta, or open-delta configuration, and is followed by a transmission line. Fig. 1b provides a schematic where overall SVR connection is modeled as a series element between nodes n and m. The secondary of the autotransformer bank is denoted by n', and is by convention not included in the set $\mathcal{N}$. The transmission line is connected between n' and m.

The relationship between the voltages across the SVR $(n,m) \in \mathcal{E}_{\rm R}$ is $\mathbf{v}_n = \mathbf{A}_{nm}\mathbf{v}_{n'}$ where $\mathbf{A}_{nm}$ is the voltage gain matrix and depends on the tap position. The tap position determines the effective turns ratios of the autotransformer bank. For $(n,m) \in \mathcal{E}_{\rm R}$, the vector of effective turns ratios for wye, closed-delta, and open-delta SVRs is respectively denoted by $\mathbf{r}_{nm} := \{r^a, r^b, r^c\}$, $\mathbf{r}_{nm} := \{r^{ab}, r^{bc}, r^{ca}\}$, and $\mathbf{r}_{nm} := \{r^{ab}, 1, r^{cb}\}$. The relationship between the effective turns ratio and the taps for the SVR is $r^\phi_{nm} = 1 \mp 0.00625 t^\phi_{nm}$ where t^ϕ_{nm} is an integer, ranging in 33 levels from -16 to $+16$. The plus sign is used for type-A SVRs while the minus sign is used for type-B SVRs [1]. When the tap varies between -16 to $+16$, the effective turns ratio ranges from $r_{\min} = 0.9$ to $r_{\max} = 1.1$ and assumes 33 levels. A good approximation is to consider r^ϕ_{nm} as continuous variable constrained as

$$r_{\min} \le \mathbf{r}_{nm} \le r_{\max},\ (n,m) \in \mathcal{E}_{\rm R}. \tag{2}$$

The SVR gain matrices $\mathbf{A}_{nm}$ for three main configurations have been derived in [2] and are provided in Table I, where the explicit dependence on the vector of effective turns ratios $\mathbf{r}_{nm}$ is given. For edge $(n,m) \in \mathcal{E}_{\rm R}$, the relationship between voltages and currents is as follows [2]:

$$\mathbf{i}_{nm} = \mathbf{A}^{-\top}_{nm}\mathbf{Y}^{(n)}_{nm}\mathbf{A}^{-1}_{nm}\mathbf{v}_n - \mathbf{A}^{-\top}_{nm}\mathbf{Y}^{(m)}_{nm}\mathbf{v}_m,\ (n,m) \in \mathcal{E}_{\rm R} \tag{3a}$$
$$\mathbf{i}_{mn} = \mathbf{Y}^{(m)}_{mn}\mathbf{v}_m - \mathbf{Y}^{(n)}_{mn}\mathbf{A}^{-1}_{nm}\mathbf{v}_n,\ (n,m) \in \mathcal{E}_{\rm R} \tag{3b}$$

where matrices $\mathbf{Y}$ correspond to the transmission line connecting n' to m. The relationship between $\mathbf{A}_{nm}$ and $\mathbf{r}_{nm}$ is

$$\mathbf{A}_{nm} = \mathrm{diag}(\mathbf{r}_{nm})\mathbf{D}_{nm} + \mathbf{F}_{nm},\ (n,m) \in \mathcal{E}_{\rm R} \tag{4}$$

where for wye SVRs, $\mathbf{D}_{nm} = \mathbf{I}$ and $\mathbf{F}_{nm} = \mathbf{O}$, for closed-delta SVRs $\mathbf{D}_{nm} = \left[\begin{smallmatrix} 1 & -1 & 0 \\ 0 & 1 & -1 \\ -1 & 0 & 1 \end{smallmatrix}\right]$ and $\mathbf{F}_{nm} = \left[\begin{smallmatrix} 0 & 1 & 0 \\ 0 & 0 & 1 \\ 1 & 0 & 0 \end{smallmatrix}\right]$, and for open-delta SVRs $\mathbf{D}_{nm} = \left[\begin{smallmatrix} 1 & -1 & 0 \\ 0 & 1 & 0 \\ 0 & -1 & 1 \end{smallmatrix}\right]$ and $\mathbf{F}_{nm} = \left[\begin{smallmatrix} 0 & 1 & 0 \\ 0 & 0 & 0 \\ 0 & 1 & 0 \end{smallmatrix}\right]$.

C. Power flow equations with SVRs

The power flow equations with explicit account of SVR turn ratios are presented in this section. For $\phi \in \Omega$, define the 3×1 real-valued vector $\mathbf{e}_\phi$ as $\mathbf{e}^\phi(\{\phi\}) = 1$ and $\mathbf{e}^\phi(\Omega \setminus \{\phi\}) = \mathbf{0}$; further define $\mathbf{E}^\phi = \mathbf{e}^\phi\bar{\mathbf{e}}^\phi$ and $\mathbf{E}^{\phi\phi'} = \mathbf{e}^\phi\bar{\mathbf{e}}^{\phi'}$. For a set $\mathcal{A}$, denote by $nm \in \mathcal{A}$ and $mn \in \mathcal{A}$, the sets $\{m \in \mathcal{N} | (n,m) \in \mathcal{A}\}$ and $\{m \in \mathcal{N} | (m,n) \in \mathcal{A}\}$. Compute the power injection s^ϕ_n at node $n \in \mathcal{N}$ and $\phi \in \Omega$ by

$$s^\phi_n = \bar{\mathbf{e}}^\phi\mathbf{v}_n\bar{\mathbf{i}}_n\mathbf{e}^\phi = \bar{\mathbf{i}}_n\mathbf{E}^\phi\mathbf{v}_n. \tag{5}$$

Based on KCL, the current injection $\mathbf{i}_n$ at node $n \in \mathcal{N}_+$ equals

$$\mathbf{i}_n = \sum_{nm\in\mathcal{E}} \mathbf{i}_{nm} + \sum_{mn\in\mathcal{E}} \mathbf{i}_{nm} \tag{6}$$

The appropriate terms in (1) and (3) substitute $\mathbf{i}_{nm}$ in (6) to obtain the following for $n \in \mathcal{N}$:

$$\begin{aligned}\mathbf{i}_n = &\sum_{nm,mn\in\mathcal{E}_{\rm T}} \mathbf{Y}^{(n)}_{nm}\mathbf{v}_n - \mathbf{Y}^{(m)}_{nm}\mathbf{v}_m \\ &+ \sum_{nm\in\mathcal{E}_{\rm R}} \mathbf{A}^{-\top}_{nm}\mathbf{Y}^{(n)}_{nm}\mathbf{A}^{-1}_{nm}\mathbf{v}_n - \mathbf{A}^{-\top}_{nm}\mathbf{Y}^{(m)}_{nm}\mathbf{v}_m \\ &+ \sum_{mn\in\mathcal{E}_{\rm R}} \mathbf{Y}^{(n)}_{nm}\mathbf{v}_n - \mathbf{Y}^{(m)}_{nm}\mathbf{A}^{-1}_{mn}\mathbf{v}_m.\end{aligned} \tag{7}$$

TABLE I
SVR-RELATED MATRICES

Matrices	Wye	Closed-delta	Open-delta
$\mathbf{A}_{nm}$	$\begin{bmatrix} r^a_{nm} & 0 & 0 \\ 0 & r^b_{nm} & 0 \\ 0 & 0 & r^c_{nm} \end{bmatrix}$	$\begin{bmatrix} r^{ab}_{nm} & 1-r^{ab}_{nm} & 0 \\ 0 & r^{bc}_{nm} & 1-r^{bc}_{nm} \\ 1-r^{ca}_{nm} & 0 & r^{ca}_{nm} \end{bmatrix}$	$\begin{bmatrix} r^{ab}_{nm} & 1-r^{ab}_{nm} & 0 \\ 0 & 1 & 0 \\ 0 & 1-r^{cb}_{nm} & r^{cb}_{nm} \end{bmatrix}$
$\mathbf{A}^{-1}_{nm}$	$\begin{bmatrix} \frac{1}{r^a_{nm}} & 0 & 0 \\ 0 & \frac{1}{r^b_{nm}} & 0 \\ 0 & 0 & \frac{1}{r^c_{nm}} \end{bmatrix}$	$\frac{1}{\lvert\mathbf{A}_{nm}\rvert}\begin{bmatrix} r^{bc}_{nm}r^{ca}_{nm} & -(1-r^{ab}_{nm})r^{ca}_{nm} & (1-r^{ab}_{nm})(1-r^{ca}_{nm}) \\ (1-r^{bc}_{nm})(1-r^{ca}_{nm}) & r^{ab}_{nm}r^{ca}_{nm} & -r^{ab}_{nm}(1-r^{bc}_{nm}) \\ -r^{bc}_{nm}(1-r^{ca}_{nm}) & (1-r^{ab}_{nm})(1-r^{ca}_{nm}) & r^{ab}_{nm}r^{bc}_{nm} \end{bmatrix}$	$\begin{bmatrix} \frac{1}{r^{ab}_{nm}} & 1-\frac{1}{r^{ab}_{nm}} & 0 \\ 0 & 1 & 0 \\ 0 & 1-\frac{1}{r^{cb}_{nm}} & \frac{1}{r^{cb}_{nm}} \end{bmatrix}$

Substituting (7) for $\bar{\mathbf{i}}_n$ in (5) yields the power flow equations

$$\begin{aligned} s^{\phi}_n = &\sum_{nm,mn\in\mathcal{E}_{\mathrm{T}}} \left[\overline{\mathbf{v}}_n \overline{\mathbf{Y}}^{(n)}_{nm} - \overline{\mathbf{v}}_m \overline{\mathbf{Y}}^{(m)}_{nm}\right] \mathbf{E}^{\phi}\mathbf{v}_n \\ &+ \sum_{nm\in\mathcal{E}_{\mathrm{R}}} \left[\overline{\mathbf{v}}_n \mathbf{A}^{-\top}_{nm}\overline{\mathbf{Y}}^{(n)}_{nm}\mathbf{A}^{-1}_{nm} - \overline{\mathbf{v}}_m \overline{\mathbf{Y}}^{(m)}_{nm}\mathbf{A}^{-1}_{nm}\right] \mathbf{E}^{\phi}\mathbf{v}_n \\ &- \sum_{mn\in\mathcal{E}_{\mathrm{R}}} \left[\overline{\mathbf{v}}_n \overline{\mathbf{Y}}^{(n)}_{nm} - \overline{\mathbf{v}}_m \mathbf{A}^{-\top}_{mn}\overline{\mathbf{Y}}^{(m)}_{nm}\right] \mathbf{E}^{\phi}\mathbf{v}_n, \\ &n \in \mathcal{N}, \phi \in \Omega. \end{aligned} \tag{8}$$

III. OPF WITH SVR TAP SELECTION

This section presents the OPF problem with SVR tap selection. The objective is to minimize the total power import to the distribution network, given as follows:

$$c(\mathbf{v}) = \sum_{n\in\mathcal{S}}\sum_{\phi\in\Omega} \mathrm{Re}\left[s^{\phi}_n\right] \tag{9}$$

Other cost functions that account for e.g., thermal losses, may also be included. The OPF problem is stated next.

$$\begin{aligned} \text{OPF: } \underset{\mathbf{s},\mathbf{r},\mathbf{v}}{\text{minimize}}\ & (9) \text{ subject to } (2),(4),(8), \text{ and} \\ & v_{\min} \le |\mathbf{v}| \le v_{\max} && \text{(10a)} \\ & \mathbf{v}_n = \mathbf{v}^{\mathrm{s}}_n, n \in \mathcal{S} && \text{(10b)} \\ & \mathbf{s}_n \in \mathcal{G}_n, n \in \mathcal{N}. && \text{(10c)} \end{aligned}$$

Constraint (10a) enforces lower and upper voltage magnitude bounds. Constraint (10b) specifies the voltage at the slack bus. The set $\mathcal{G}_n$ in (10c) is the feasible region of net complex power injection at bus n. In case of known distributed generation injections or loads, $\mathcal{G}_n$ is a singleton for $n \in \mathcal{N}_+$. Problem (10) is nonconvex because a) (8) is quadratic in voltages $\mathbf{v}$ and inverse quadratic in effective ratios $\mathbf{r}$, and b) the left constraint in (10a) yields a nonconvex feasible set.

IV. SEMIDEFINITE RELAXATION OF OPF WITH SVRS

This section develops a relaxation of (10). To this end, Section IV-A presents a formulation equivalent to (10), and Section IV-B develops convex relaxations. The proposed formulation is given in Section IV-C, and Section IV-D provides a method to recover a feasible solution to (10).

A. Equivalent OPF formulation

Using the identity $\sum_{\phi\in\Omega}\mathbf{E}^{\phi} = \mathbf{I}$, we have that

$$\mathbf{A}^{-1}_{nm} = \mathbf{A}^{-1}_{nm}\sum_{\phi'\in\Omega}\mathbf{E}^{\phi'}. \tag{11}$$

Consider the change of variables of the following form:

$$\mathbf{u}^{\phi}_{nm} = \mathbf{A}^{-1}_{nm}\mathbf{E}^{\phi}\mathbf{v}_n, (n,m) \in \mathcal{E}_{\mathrm{R}}, \phi \in \Omega, \tag{12}$$

and collect all such variables in the vector $\mathbf{u}$. By incorporating (11) in (8) and using the cyclic permutation property of the trace operator and subsequently substituting in (12), the OPF (10) is equivalently written as

$$\begin{aligned} \text{EOPF: } \underset{\mathbf{s},\mathbf{r},\mathbf{v},\mathbf{u}}{\text{minimize}}\ & (9) \\ \text{subject to } & (2),(4),(10a),(10b),(10c),(12) \\ s^{\phi}_n = &\sum_{nm,mn\in\mathcal{E}_{\mathrm{T}}} \mathrm{Tr}\left[\overline{\mathbf{Y}}^{(n)}_{nm}\mathbf{E}^{\phi}\mathbf{v}_n\overline{\mathbf{v}}_n - \overline{\mathbf{Y}}^{(m)}_{nm}\mathbf{E}^{\phi}\mathbf{v}_n\overline{\mathbf{v}}_m\right] \\ &+ \sum_{nm\in\mathcal{E}_{\mathrm{R}}}\sum_{\phi'\in\Omega} \mathrm{Tr}\left[\overline{\mathbf{Y}}^{(n)}_{nm}\mathbf{u}^{\phi}_{nm}\overline{\mathbf{u}}^{\phi'}_{nm}\right] \\ &- \sum_{nm\in\mathcal{E}_{\mathrm{R}}} \mathrm{Tr}\left[\overline{\mathbf{Y}}^{(m)}_{nm}\mathbf{u}^{\phi}_{nm}\overline{\mathbf{v}}_m\right] \\ &+ \sum_{mn\in\mathcal{E}_{\mathrm{R}}} \mathrm{Tr}\left[\overline{\mathbf{Y}}^{(n)}_{nm}\mathbf{E}^{\phi}\mathbf{v}_n\overline{\mathbf{v}}_n\right] \\ &- \sum_{mn\in\mathcal{E}_{\mathrm{R}}}\sum_{\phi'\in\Omega} \mathrm{Tr}\left[\overline{\mathbf{Y}}^{(m)}_{nm}\mathbf{E}^{\phi}\mathbf{v}_n\overline{\mathbf{u}}^{\phi'}_{mn}\right], \\ &n \in \mathcal{N}, \phi \in \Omega. \end{aligned} \tag{13a}$$

The following new variables are introduced:

$$\begin{aligned} &\mathbf{W}_{nn} = \mathbf{v}_n\overline{\mathbf{v}}_n, n \in \mathcal{N}, \mathbf{W}_{nm} = \mathbf{v}_n\overline{\mathbf{v}}_m, (n,m) \in \mathcal{E}_{\mathrm{T}} && \text{(14)} \\ &\mathbf{U}^{\phi\phi'}_{nm} = \mathbf{u}^{\phi}_{nm}\overline{\mathbf{u}}^{\phi'}_{nm}, (n,m) \in \mathcal{E}_{\mathrm{R}}, \phi, \phi' \in \Omega && \text{(15a)} \\ &\mathbf{\Psi}^{\phi}_{nm} = \mathbf{u}^{\phi}_{nm}\overline{\mathbf{v}}_m, (n,m) \in \mathcal{E}_{\mathrm{R}}, \phi \in \Omega && \text{(15b)} \\ &\mathbf{U}_{nm} = [\{\mathbf{U}^{\phi,\phi'}_{nm}\}_{\phi'\in\Omega}]_{\phi\in\Omega}, (n,m) \in \mathcal{E}_{\mathrm{R}} && \text{(16a)} \\ &\mathbf{\Psi}_{nm} = \{\mathbf{\Psi}^{\phi}_{nm}\}_{\phi\in\Omega}, (n,m) \in \mathcal{E}_{\mathrm{R}}. && \text{(16b)} \end{aligned}$$

In (16), the notation [.] is a horizontal concatenation of matrices. Collect $\mathbf{U}_{nm}$ and $\mathbf{\Psi}_{nm}$ for $(n,m) \in \mathcal{E}_{\mathrm{R}}$ respectively in $\mathbf{U}$

Algorithm 1 Retrieve $\mathbf{v}, \mathbf{u}$ from $(\mathbf{W}, \mathbf{U}, \mathbf{\Psi})$

Initialize $\mathcal{N}_{\rm visit} \leftarrow \{\rm S\}$ and $\mathbf{v}_{\rm S} = \mathbf{v}_{\rm S}^{\rm s}$.
while $\mathcal{N}_{\rm visit} \neq \mathcal{N}$ **do**
  Find $(n,m) \in \mathcal{E}$ such that $n \in \mathcal{N}_{\rm visit}$ and $m \notin \mathcal{N}_{\rm visit}$.
  if $m : (n,m) \in \mathcal{E}_{\rm R}$ **then**
    $\mathbf{u}_{nm}^{\phi} \leftarrow \mathbf{A}_{nm}^{-1}\mathbf{E}^{\phi}\mathbf{v}_n, \phi \in \Omega_n$ $\mathbf{u}_{nm} \leftarrow \{\mathbf{u}_{nm}^{\phi}\}_{\phi\in\Omega_n}$
    $\mathbf{v}_m \leftarrow \overline{\mathbf{\Psi}}_{nm}\mathbf{u}_{nm}/\operatorname{Tr}[\mathbf{U}_{nm}]$
  else
    $\mathbf{v}_m \leftarrow \overline{\mathbf{W}}_{nm}\mathbf{v}_n/\operatorname{Tr}[\mathbf{W}_{nn}]$
  end if
  Update $\mathcal{N}_{\rm visit} \leftarrow \mathcal{N}_{\rm visit} \cup \{m\}$.
end while

and $\mathbf{\Psi}$; and likewise collect $\mathbf{W}_{nn}$ and $\mathbf{W}_{nm}$ for $(n,m) \in \mathcal{E}_{\rm T}$ in $\mathbf{W}$. We introduce the following rank-constrained OPF:

$$\text{ROPF: } \underset{\substack{\mathbf{s},\mathbf{r},\mathbf{W},\\ \mathbf{U},\mathbf{\Psi}}}{\text{minimize}} \sum_{n\in\mathcal{S}}\sum_{\phi\in\Omega_n} \operatorname{Re}\left[s_n^{\phi}\right] \tag{17a}$$

$$\text{subject to } (2),(4),(10c),(16)$$

$$(v^{\min})^2 \le \operatorname{diag}(\mathbf{W}) \le (v^{\max})^2 \tag{17b}$$

$$\mathbf{W}_{nn} = \mathbf{v}_n^{\rm s}\overline{\mathbf{v}}_n^{\rm s}, n \in \mathcal{S} \tag{17c}$$

$$\begin{aligned} s_n^{\phi} = &\sum_{nm,mn\in\mathcal{E}_{\rm T}} \operatorname{Tr}\left[\overline{\mathbf{Y}}_{nm}^{(n)}\mathbf{E}^{\phi}\mathbf{W}_{nn} - \overline{\mathbf{Y}}_{nm}^{(m)}\mathbf{E}^{\phi}\mathbf{W}_{nm}\right] \\ &+ \sum_{nm\in\mathcal{E}_{\rm R}}\sum_{\phi'\in\Omega} \operatorname{Tr}\left[\overline{\mathbf{Y}}_{nm}^{(n)}\mathbf{U}_{nm}^{\phi\phi'}\right] \\ &- \sum_{nm\in\mathcal{E}_{\rm R}} \operatorname{Tr}\left[\overline{\mathbf{Y}}_{nm}^{(m)}\mathbf{\Psi}_{nm}^{\phi}\right] \\ &+ \sum_{mn\in\mathcal{E}_{\rm R}} \operatorname{Tr}\left[\overline{\mathbf{Y}}_{nm}^{(n)}\mathbf{E}_n^{\phi}\mathbf{W}_{nn}\right] \\ &- \sum_{mn\in\mathcal{E}_{\rm R}}\sum_{\phi'\in\Omega} \operatorname{Tr}\left[\overline{\mathbf{Y}}_{nm}^{(m)}\mathbf{E}_n^{\phi}\overline{\mathbf{\Psi}}_{mn}^{\phi'}\right], n \in \mathcal{N}, \phi \in \Omega \end{aligned} \tag{17d}$$

$$\begin{bmatrix}\mathbf{W}_{nn} & \mathbf{W}_{nm}\\ \overline{\mathbf{W}}_{nm} & \mathbf{W}_{mm}\end{bmatrix} \succeq \mathbf{O}, (n,m) \in \mathcal{E}_{\rm T} \tag{17e}$$

$$\begin{bmatrix}\mathbf{U}_{nm} & \mathbf{\Psi}_{nm}\\ \overline{\mathbf{\Psi}}_{nm} & \mathbf{W}_{mm}\end{bmatrix} \succeq \mathbf{O}, (n,m) \in \mathcal{E}_{\rm R} \tag{17f}$$

$$\operatorname{Rank}\begin{bmatrix}\mathbf{W}_{nn} & \mathbf{W}_{nm}\\ \overline{\mathbf{W}}_{nm} & \mathbf{W}_{mm}\end{bmatrix} = 1, (n,m) \in \mathcal{E}_{\rm T} \tag{17g}$$

$$\operatorname{Rank}\begin{bmatrix}\mathbf{U}_{nm} & \mathbf{\Psi}_{nm}\\ \overline{\mathbf{\Psi}}_{nm} & \mathbf{W}_{mm}\end{bmatrix} = 1, (n,m) \in \mathcal{E}_{\rm R} \tag{17h}$$

$$\mathbf{U}_{nm}^{\phi\phi'} = \mathbf{A}_{nm}^{-1}\mathbf{E}^{\phi}\mathbf{W}_{nn}\mathbf{E}^{\phi'}\mathbf{A}_{nm}^{-\top}, (n,m) \in \mathcal{E}_{\rm R}, \phi, \phi' \in \Omega. \tag{17i}$$

In (17), the nonconvex constraints are (17g), (17h), and (17i). If the matrices in (17g), (17h), and (17i) are rank-1, spectral decomposition renders voltages of problem (10).

Lemma 1. *Suppose that graph $(\mathcal{N},\mathcal{E})$ is radial with one slack bus $\mathcal{S} = \{\rm S\}$ and the point $(\mathbf{s}^*, \mathbf{r}^*, \mathbf{W}^*, \mathbf{U}^*, \mathbf{\Psi}^*)$ is an optimal solution of* (17)*. Then, the point $(\mathbf{s}^*, \mathbf{r}^*, \mathbf{v}^*, \mathbf{u}^*)$, where $\mathbf{v}^*$ and $\mathbf{u}^*$ are computed via Algorithm 1, is an optimal point of* (13)*.*

Proof: The proof is similar to [4, Lemma 1], but extended to handle SVR branches. We omit it here to preserve space. ■

B. Convex relaxation

To derive a convex relaxation of (17), (17g) and (17h) can be dropped. Constraint (17i) is more challenging to handle since $\mathbf{A}_{nm}$ depends linearly on the optimization vector $\mathbf{r}$ through (4), but the inverse of $\mathbf{A}_{nm}$ appears in (17i).

An equivalent but more amenable form of (17i) is developed next, before the constraint can be relaxed to a convex one. Let $W_{nn}^{\phi\phi'}$ be the entry of $\mathbf{W}_{nn}$ corresponding to phase pair (ϕ,ϕ') (cf. (14)). The next proposition gives an equivalent constraint to (17i) that does not include the inverse of $\mathbf{A}_{nm}$.

Proposition 1. *Constraint* (17i) *is equivalent to*

$$\begin{aligned} W_{nn}^{\phi\phi'}\mathbf{E}^{\phi\phi'} = &\operatorname{diag}(\mathbf{r}_{nm})\mathbf{D}_{nm}\mathbf{U}_{nm}^{\phi\phi'}\mathbf{D}_{nm}^{\top}\operatorname{diag}(\mathbf{r}_{nm}) \\ &+ \operatorname{diag}(\mathbf{r}_{nm})\mathbf{D}_{nm}\mathbf{U}_{nm}^{\phi\phi'}\mathbf{F}_{nm}^{\top} \\ &+ \mathbf{F}_{nm}\mathbf{U}_{nm}^{\phi\phi'}\mathbf{D}_{nm}^{\top}\operatorname{diag}(\mathbf{r}_{nm}) \\ &+ \mathbf{F}_{nm}\mathbf{U}_{nm}^{\phi\phi'}\mathbf{F}_{nm}^{\top}, (n,m) \in \mathcal{E}_{\rm R},\ \phi,\phi' \in \Omega. \end{aligned} \tag{18}$$

Proof: Since $\mathbf{A}_{nm}$ is invertible for all three types of SVR in Table I [2], constraint (17i) can be written equivalently as

$$\mathbf{A}_{nm}\mathbf{U}_{nm}^{\phi\phi'}\mathbf{A}_{nm}^{\top} = \mathbf{E}^{\phi}\mathbf{W}_{nn}\mathbf{E}^{\phi'} = W_{nn}^{\phi\phi'}\mathbf{E}^{\phi\phi'}. \tag{19}$$

Introducing (4) in (19) yields (18). ■

Eq. (18) is nonconvex, as the product of variables $\mathbf{r}_{nm}$ and $\mathbf{U}_{nm}$ enters an equality constraint. To convexify (18), we first drop its off-diagonals ($\phi \neq \phi'$). We then focus on the diagonal entries of (18), which have the form

$$\alpha_{nm}^{\phi'\phi}(r_{nm}^{\phi})^2 + 2\beta_{nm}^{\phi'\phi}r_{nm}^{\phi} + \kappa_{nm}^{\phi'\phi} = 0, \phi' \neq \phi \in \Omega, \tag{20a}$$

$$\alpha_{nm}^{\phi\phi}(r_{nm}^{\phi})^2 + 2\beta_{nm}^{\phi\phi}r_{nm}^{\phi} + \kappa_{nm}^{\phi\phi} = W_{nn}^{\phi\phi}, \phi \in \Omega \tag{20b}$$

where $\alpha_{nm}^{\phi'\phi}$, $\beta_{nm}^{\phi'\phi}$, and $\kappa_{nm}^{\phi'\phi}$ are defined as the ϕ-th element on the diagonals of $\mathbf{D}_{nm}\mathbf{U}_{nm}^{\phi'\phi'}\mathbf{D}_{nm}^{\top}$, $\operatorname{Re}\left[\mathbf{D}_{nm}\mathbf{U}_{nm}^{\phi'\phi'}\mathbf{F}_{nm}^{\top}\right]$, and $\mathbf{F}_{nm}\mathbf{U}_{nm}^{\phi'\phi'}\mathbf{F}_{nm}^{\top}$, respectively. Notice that $\alpha_{nm}^{\phi'\phi}$, $\beta_{nm}^{\phi'\phi}$, and $\kappa_{nm}^{\phi'\phi}$ are linear functions of $\mathbf{U}_{nm}^{\phi'\phi'}$. For convenience, matrices $\mathbf{D}_{nm}\mathbf{U}_{nm}^{\phi'\phi'}\mathbf{D}_{nm}^{\top}$ and $\mathbf{D}_{nm}\mathbf{U}_{nm}^{\phi'\phi'}\mathbf{F}_{nm}^{\top}$, and $\mathbf{F}_{nm}\mathbf{U}_{nm}^{\phi'\phi'}\mathbf{F}_{nm}^{\top}$ for a generic $\mathbf{U}_{nm}^{\phi'\phi'} = \begin{bmatrix}U_{nm}^{11} & U_{nm}^{12} & U_{nm}^{13}\\ U_{nm}^{21} & U_{nm}^{22} & U_{nm}^{23}\\ U_{nm}^{31} & U_{nm}^{32} & U_{nm}^{33}\end{bmatrix}$ are provided in Table II for each SVR type. It will be notationally convenient to derive the relaxations specifically according to the SVR type. To this end, the next three sections describe how (20) is relaxed depending on SVR type. In what follows, we partition $\mathcal{E}_{\rm R}$ as $\mathcal{E}_{\rm R} = \mathcal{E}_{\rm Y} \cup \mathcal{E}_{\rm C} \cup \mathcal{E}_{\rm O}$, where $\mathcal{E}_{\rm Y}$, $\mathcal{E}_{\rm C}$, and $\mathcal{E}_{\rm O}$ respectively collect wye, closed-delta, and open-delta SVR edges.

1) Wye SVRs: For wye SVRs, a linear substitute of (20a) is provided next.

Proposition 2. *For $(n,m) \in \mathcal{E}_{\rm Y}$,* (20a) *is equivalent to*

$$\alpha_{nm}^{\phi'\phi} = 0, \phi' \neq \phi \in \Omega. \tag{21}$$

Proof: From Table II, $\alpha_{nm}^{\phi'\phi} = U_{nm}^{\phi\phi}$ while the values of $\beta_{nm}^{\phi'\phi}$ and $\kappa_{nm}^{\phi'\phi}$ which are the diagonals of matrices $\mathbf{D}_{nm}\mathbf{U}_{nm}^{\phi'\phi'}\mathbf{F}_{nm}$ equate to zero. Then, (20a) reduces to $U_{nm}^{\phi\phi}(r_{nm}^{\phi})^2 = 0$. The latter equality is equivalent to (21) since $r_{nm}^{\phi} \in [r_{\min}, r_{\max}]$ where $r_{\min} > 0$. ■

For wye SVRs, (20b) is linearly relaxed next.

TABLE II
SVR-RELATED MATRIX COMPUTATIONS

Matrices	Wye	Closed-delta	Open-delta
$\mathbf{D}_{nm}\mathbf{U}_{nm}^{\phi'\phi}\mathbf{D}_{nm}^{\top}$	$\begin{bmatrix} U_{nm}^{11} & U_{nm}^{12} & U_{nm}^{13} \\ U_{nm}^{21} & U_{nm}^{22} & U_{nm}^{23} \\ U_{nm}^{31} & U_{nm}^{32} & U_{nm}^{33} \end{bmatrix}$	$\begin{bmatrix} U_{nm}^{11}+U_{nm}^{22} & U_{nm}^{12}+U_{nm}^{23} & U_{nm}^{13}+U_{nm}^{21} \\ -2\mathrm{Re}[U_{nm}^{12}] & -U_{nm}^{22}-U_{nm}^{13} & -U_{nm}^{11}-U_{nm}^{23} \\ U_{nm}^{21}+U_{nm}^{32} & U_{nm}^{22}+U_{nm}^{33} & U_{nm}^{31}+U_{nm}^{23} \\ -U_{nm}^{31}-U_{nm}^{22} & -2\mathrm{Re}[U_{nm}^{23}] & -U_{nm}^{33}-U_{nm}^{21} \\ U_{nm}^{31}+U_{nm}^{12} & U_{nm}^{32}+U_{nm}^{13} & U_{nm}^{33}+U_{nm}^{11} \\ -U_{nm}^{11}-U_{nm}^{32} & -U_{nm}^{12}-U_{nm}^{33} & -2\mathrm{Re}[U_{nm}^{31}] \end{bmatrix}$	$\begin{bmatrix} U_{nm}^{11}+U_{nm}^{22} & U_{nm}^{12}-U_{nm}^{22} & U_{nm}^{13}+U_{nm}^{22} \\ -2\mathrm{Re}[U_{nm}^{12}] & & -U_{nm}^{23}-U_{nm}^{12} \\ U_{nm}^{21}-U_{nm}^{22} & U_{nm}^{22} & U_{nm}^{23}-U_{nm}^{22} \\ U_{nm}^{31}+U_{nm}^{22} & U_{nm}^{32}-U_{nm}^{22} & U_{nm}^{33}+U_{nm}^{22} \\ -U_{nm}^{21}-U_{nm}^{32} & & -2\mathrm{Re}[U_{nm}^{23}] \end{bmatrix}$
$\mathbf{D}_{nm}\mathbf{U}_{nm}^{\phi'\phi'}\mathbf{F}_{nm}^{\top}$	$\mathbf{O}$	$\begin{bmatrix} U_{nm}^{12}-U_{nm}^{22} & U_{nm}^{13}-U_{nm}^{23} & U_{nm}^{11}-U_{nm}^{21} \\ U_{nm}^{22}-U_{nm}^{32} & U_{nm}^{23}-U_{nm}^{33} & U_{nm}^{21}-U_{nm}^{31} \\ U_{nm}^{32}-U_{nm}^{12} & U_{nm}^{33}-U_{nm}^{13} & U_{nm}^{32}-U_{nm}^{11} \end{bmatrix}$	$\begin{bmatrix} U_{nm}^{12}-U_{nm}^{22} & 0 & U_{nm}^{12}-U_{nm}^{22} \\ U_{nm}^{22} & 0 & U_{nm}^{22} \\ U_{nm}^{32}-U_{nm}^{22} & 0 & U_{nm}^{32}-U_{nm}^{22} \end{bmatrix}$
$\mathbf{F}_{nm}\mathbf{U}_{nm}^{\phi'\phi'}\mathbf{F}_{nm}^{\top}$	$\mathbf{O}$	$\begin{bmatrix} U_{nm}^{22} & U_{nm}^{23} & U_{nm}^{21} \\ U_{nm}^{32} & U_{nm}^{33} & U_{nm}^{31} \\ U_{nm}^{12} & U_{nm}^{13} & U_{nm}^{11} \end{bmatrix}$	$\begin{bmatrix} U_{nm}^{22} & 0 & U_{nm}^{22} \\ 0 & 0 & 0 \\ U_{nm}^{22} & 0 & U_{nm}^{22} \end{bmatrix}$

Proposition 3. *For* $(n,m) \in \mathcal{E}_{\mathrm{Y}}$, (20b) *implies*

$$\alpha_{nm}^{\phi\phi} r_{\min}^2 \leq W_{nn}^{\phi\phi} \leq \alpha_{nm}^{\phi\phi} r_{\max}^2, \phi \in \Omega. \tag{22}$$

Proof: From Table II, it holds that $\alpha_{nm}^{\phi\phi} = U_{nm}^{\phi\phi}$ while the values of $\beta_{nm}^{\phi\phi}$ and $\kappa_{nm}^{\phi\phi}$ which are the diagonals of matrices $\mathbf{D}_{nm}\mathbf{U}_{nm}^{\phi\phi}\mathbf{F}_{nm}$ equate to zero. Hence, (20b) reduces to $U_{nm}^{\phi\phi}(r_{nm}^{\phi})^2 = W_{nn}^{\phi\phi}$. The latter equality implies (22) since $r_{nm}^{\phi} \in [r_{\min}, r_{\max}]$ where $r_{\min} > 0$ and $U_{nm}^{\phi\phi} \geq 0$ (due to positive semidefiniteness of $\mathbf{U}_{nm}^{\phi\phi}$). ∎

2) Closed-delta SVRs: For closed-delta SVRs, (20a) is linearly relaxed next.

Proposition 4. *For* $(n,m) \in \mathcal{E}_{\mathrm{C}}$, (20a) *implies*

$$\alpha_{nm}^{\phi'\phi} r_{\min} + \beta_{nm}^{\phi'\phi} \leq 0, \phi' \neq \phi \in \Omega \tag{23a}$$
$$\alpha_{nm}^{\phi'\phi} r_{\max} + \beta_{nm}^{\phi'\phi} \geq 0, \phi' \neq \phi \in \Omega \tag{23b}$$
$$\beta_{nm}^{\phi'\phi} r_{\min} + \kappa_{nm}^{\phi'\phi} \geq 0, \phi' \neq \phi \in \Omega \tag{23c}$$
$$\beta_{nm}^{\phi'\phi} r_{\max} + \kappa_{nm}^{\phi'\phi} \leq 0, \phi' \neq \phi \in \Omega. \tag{23d}$$

Proof: We prove Proposition 4 only for $\phi' = a$ and $\phi = b$. First, notice that since $\mathbf{U}_{nm}^{aa}$ is rank-1 and positive-semidefinite, it holds that $\mathbf{U}_{nm}^{aa} = \mathbf{u}_{nm}^{a}\overline{\mathbf{u}}_{nm}^{a}$ for some vector $\mathbf{u}_{nm}^{a} = \left[u_{nm}^{a1}, u_{nm}^{a2}, u_{nm}^{a3}\right]^{\top}$. Further, since $\mathbf{W}_{nn}$ is rank-1 and positive semidefinite, it holds that $\mathbf{W}_{nn} = \mathbf{v}_n\overline{\mathbf{v}}_n$. Through (17i), we next find that $\mathbf{u}_{nm}^{a} = v_n^a\left[\mathbf{A}_{nm}^{-1}\right]_{\bullet a}$, where $\left[\mathbf{A}_{nm}^{-1}\right]_{\bullet a}$ denotes the a-th column of $\mathbf{A}_{nm}^{-1}$. The latter equality and Table I then aid in finding $\mathbf{u}_{nm}^{a}$:

$$u_{nm}^{a1} = v_n^a\left[\mathbf{A}_{nm}^{-1}\right]_{1a} = v_n^a\frac{r_{nm}^{bc}r_{nm}^{ca}}{|\mathbf{A}_{nm}|} \tag{24a}$$
$$u_{nm}^{a2} = v_n^a\left[\mathbf{A}_{nm}^{-1}\right]_{2a} = v_n^a\frac{(1-r_{nm}^{bc})(1-r_{nm}^{ca})}{|\mathbf{A}_{nm}|} \tag{24b}$$
$$u_{nm}^{a3} = v_n^a\left[\mathbf{A}_{nm}^{-1}\right]_{3a} = v_n^a\frac{-r_{nm}^{bc}(1-r_{nm}^{ca})}{|\mathbf{A}_{nm}|}. \tag{24c}$$

Assume $\phi = b$. Using (24) and Table II, compute the following quantities by noting that when $\phi = b$, then $r_{nm}^{\phi} = r_{nm}^{bc}$.

$$\alpha_{nm}^{ab} = U_{nm}^{22} + U_{nm}^{33} - 2\mathrm{Re}[U_{nm}^{32}] = \left|u_{nm}^{a2} - u_{nm}^{a3}\right|^2$$
$$\Rightarrow \alpha_{nm}^{ab} = \frac{|v_n^a|^2}{|\mathbf{A}_{nm}|^2}(1-r_{nm}^{ca})^2 \tag{24d}$$
$$\beta_{nm}^{ab} = \mathrm{Re}[U_{nm}^{23}] - U_{nm}^{33} = \mathrm{Re}\left[(u_{nm}^{a2} - u_{nm}^{a3})\overline{u}_{nm}^{a3}\right]$$
$$\Rightarrow \beta_{nm}^{ab} = -\frac{|v_n^a|^2}{|\mathbf{A}_{nm}|^2}r_{nm}^{bc}(1-r_{nm}^{ca})^2 \tag{24e}$$
$$\kappa_{nm}^{ab} = U_{nm}^{33} = |u_{nm}^{a3}|^2 = \frac{|v_n^a|^2}{|\mathbf{A}_{nm}|^2}(r_{nm}^{bc})^2(1-r_{nm}^{ca})^2. \tag{24f}$$

It thus holds that

$$\alpha_{nm}^{ab} r_{nm}^{bc} + \beta_{nm}^{ab} = 0. \tag{25}$$

The above equality together with the fact that $\alpha_{nm}^{ab} \geq 0$ imply (23a) and (23b) for $\phi' = a$ and $\phi = b$. Equation (25) with the fact that $\beta_{nm}^{ab} \leq 0$ imply (23c) and (23d), for $\phi' = a$ and $\phi = b$. Other values of ϕ' and ϕ are similarly proved. ∎

For closed-delta SVRs, (20b) is linearly relaxed next.

Proposition 5. *For* $(n,m) \in \mathcal{E}_{\mathrm{C}}$, (20b) *implies*

$$\alpha_{nm}^{\phi\phi} r_{\min} + \beta_{nm}^{\phi\phi} \geq 0, \phi \in \Omega \tag{26a}$$
$$\alpha_{nm}^{\phi\phi}(r_{\min})^2 + \beta_{nm}^{\phi\phi} r_{\min} + \kappa_{nm}^{\phi\phi} \leq W_{nn}^{\phi\phi}, \phi \in \Omega \tag{26b}$$
$$\alpha_{nm}^{\phi\phi}(r_{\max})^2 + \beta_{nm}^{\phi\phi} r_{\max} + \kappa_{nm}^{\phi\phi} \geq W_{nn}^{\phi\phi}, \phi \in \Omega. \tag{26c}$$

Proof: We prove Proposition 5 only for $\phi = a$. Using (24) and Table II, we compute the following quantities by noting that when $\phi = a$, then $r_{nm}^{\phi} = r_{nm}^{ab}$.

$$\alpha_{nm}^{aa} = \frac{|v_n^a|^2}{|\mathbf{A}_{nm}|^2}(r_{nm}^{bc} + r_{nm}^{ca} - 1)^2 \tag{27a}$$
$$\beta_{nm}^{aa} = \frac{|v_n^a|^2}{|\mathbf{A}_{nm}|^2}(r_{nm}^{bc} + r_{nm}^{ca} - 1)(1-r_{nm}^{bc})(1-r_{nm}^{ca}) \tag{27b}$$
$$\kappa_{nm}^{aa} = \frac{|v_n^a|^2}{|\mathbf{A}_{nm}|^2}(1-r_{nm}^{bc})^2(1-r_{nm}^{ca})^2. \tag{27c}$$

Hence, it holds that

$$\alpha_{nm}^{aa} r_{nm}^{ab} + \beta_{nm}^{aa} = \frac{|v_n^a|^2}{|\mathbf{A}_{nm}|}(r_{nm}^{bc} + r_{nm}^{ca} - 1)\cdot \left[r_{nm}^{ab}(r_{nm}^{bc} + r_{nm}^{ca} - 1) + (1-r_{nm}^{bc})(1-r_{nm}^{ca})\right]. \tag{28}$$

In (28), the term in brackets is nonnegative due to the result of Lemma 2. Therefore, since r_{nm}^{bc} and r_{nm}^{ca} are greater than $\frac{1}{2}$, it then holds that

$$\alpha_{nm}^{aa} r_{nm}^{ab} + \beta_{nm}^{aa} \geq 0. \tag{29}$$

Equation (29) implies (26a) for $\phi = a$. Next, in order to prove (26b) and (26c) we first bring to attention that in (27a) and (27b), the values of α_{nm}^{aa} and β_{nm}^{aa} are not dependent on r_{nm}^{ab} and are non-negative. Hence, (29) implies that the derivative of the following function is non-negative:

$$g(r_{nm}^{ab}) := \alpha_{nm}^{aa}(r_{nm}^{ab})^2 + \beta_{nm}^{aa} r_{nm}^{ab} + \kappa_{nm}^{aa} - W_{nn}^{\phi\phi}. \tag{30}$$

It thus holds that $g(r_{nm}^{ab})$ is a non-decreasing function of r_{nm}^{ab} in the interval $[r_{\min}, r_{\max}]$, which implies (26b) and (26c). ■

Lemma 2. *For real numbers r^{ab}, r^{bc}, r^{ca} in the interval $[r_{\min}, r_{\max}]$ where $r_{\max} - (r_{\min})^2 \leq \frac{1}{3}$, it hold that*

$$r^{ab}(r^{bc} + r^{ca} - 1) + (1 - r^{bc})(1 - r^{ca}) \geq 0. \tag{31}$$

Proof: Expanding (31) yields

$$r^{ab}r^{bc} + r^{ab}r^{ca} + r^{bc}r^{ca} + 1 - r^{ab} - r^{bc} - r^{ca}$$
$$\geq 3(r_{\min})^2 + 1 - 3r_{\max} = 1 - 3(r_{\max} - (r_{\min})^2) \geq 0. \quad ■$$

3) Open-delta SVRs: Due to similarity to the previous section, the proofs are omitted here. The next proposition is an equivalent form of (20a) when $\phi' = a$ or $\phi' = c$.

Proposition 6. *For $(n,m) \in \mathcal{E}_{\rm O}$, $\phi' \in \{a, c\}$ and $\phi \in \{b, c\}$,* (20a) *is equivalent to*

$$\alpha_{nm}^{\phi'\phi} = 0, \beta_{nm}^{\phi'\phi} = 0, \kappa_{nm}^{\phi'\phi} = 0, \phi' \neq \phi \in \Omega. \tag{32}$$

For open-delta SVRs, (20a) for $\phi' = b$ is relaxed next.

Proposition 7. *For $(n,m) \in \mathcal{E}_{\rm O}$, $\phi' = b$ and $\phi \in \{a, c\}$,* (20a) *implies*

$$\alpha_{nm}^{b\phi} r_{\min} + \beta_{nm}^{b\phi} \leq 0, \alpha_{nm}^{b\phi} r_{\max} + \beta_{nm}^{b\phi} \geq 0 \tag{33a}$$
$$\beta_{nm}^{b\phi} r_{\min} + \kappa_{nm}^{b\phi} \geq 0, \beta_{nm}^{b\phi} r_{\max} + \kappa_{nm}^{b\phi} \leq 0. \tag{33b}$$

For open-delta SVRs, (20b) is linearly relaxed next.

Proposition 8. *For $(n,m) \in \mathcal{E}_{\rm O}$, $\phi \in \{a, c\}$,* (20b) *implies*

$$\alpha_{nm}^{\phi\phi} r_{\min}^2 \leq W_{nn}^{\phi\phi} \leq \alpha_{nm}^{\phi\phi} r_{\max}^2, \phi \in \Omega \tag{34a}$$
$$\beta_{nm}^{\phi\phi} = 0, \kappa_{nm}^{\phi\phi} = 0, \phi \in \Omega, \tag{34b}$$

In this proposition, for $\phi = b$, we assume $r_{\min} = r_{\max} = 1$.

C. Semidefinite relaxation of OPF

The proposed semidefinite relaxation of OPF is

$$\begin{aligned} &\text{SOPF: } \underset{\mathbf{s},\mathbf{W},\mathbf{U},\mathbf{\Psi}}{\text{minimize}}\ (9) \\ &\text{subject to } (10c), (16), (17b)\text{–}(17f) \\ &(21), (22)\ (n,m) \in \mathcal{E}_{\rm Y}, (23), (26)\ (n,m) \in \mathcal{E}_{\rm C} \\ &(32), (33), (34)\ (n,m) \in \mathcal{E}_{\rm O}. \end{aligned} \tag{35}$$

D. Feasible solution

After solving (35), the effective turns ratios r_{nm}^{ϕ} for $\phi \in \Omega$ can be recovered by solving (20b)—a quadratic equality in r_{nm}^{ϕ}. That a solution r_{nm}^{ϕ} exists in $[r_{\min}, r_{\max}]$ is proven next.

Proposition 9. *If $\mathbf{U}_{nm}$ and $\mathbf{W}_{nn}$ are feasible for* (35)*, then* (20b) *has a unique solution r_{nm}^{ϕ} in the range $[r_{\min}, r_{\max}]$.*

Proof: Respectively for $(n,m) \in \mathcal{E}_{\rm Y}$ and $(n,m) \in \mathcal{E}_{\rm O}$, propositions 3 and 8 imply that (20b) reduces to the form

$$g(r_{nm}^{\phi}) := \alpha_{nm}^{\phi\phi}(r_{nm}^{\phi})^2 - W_{nn}^{\phi\phi} = 0. \tag{36}$$

Respectively for $(n,m) \in \mathcal{E}_{\rm Y}$ and $(n,m) \in \mathcal{E}_{\rm O}$, however, (22) and (34a) imply that $g(r_{\min}) \leq 0$ and $g(r_{\max}) \geq 0$. The intermediate value theorem is invoked to prove that one zero crossing exists at a point $r_{nm}^{\phi} \in [r_{\min}, r_{\max}]$. Since $r_{\min} > 0$, the only valid solution to (36) is thus $r_{nm}^{\phi} = \sqrt{\frac{W_{nn}^{\phi\phi}}{\alpha_{nm}^{\phi\phi}}}$.

For $(n,m) \in \mathcal{E}_{\rm C}$, (20b) is of the form

$$g^{\rm c}(r_{nm}^{\phi}) := \alpha_{nm}^{\phi\phi}(r_{nm}^{\phi})^2 + 2\beta_{nm}^{\phi} r_{nm}^{\phi} + \kappa_{nm}^{\phi} - W_{nn}^{\phi\phi} = 0, \tag{37}$$

Equations (26b) and (26c), however, imply that $g^{\rm c}(r_{\min}) \leq 0$ and $g^{\rm c}(r_{\max}) \geq 0$. The intermediate value theorem is then invoked to prove that at least one solution $r_{nm}^{\phi} \in [r_{\min}, r_{\max}]$ exists. Equation (26a) further requires that $\alpha_{nm}^{\phi\phi} r_{nm}^{\phi} + \beta_{nm}^{\phi\phi} \geq 0$ so that the only viable solution to (37) is

$$r_{nm}^{\phi} = \frac{1}{\alpha_{nm}^{\phi\phi}} \left[-\beta_{nm}^{\phi\phi} + \sqrt{(\beta_{nm}^{\phi\phi})^2 - \alpha_{nm}^{\phi\phi}(\kappa_{nm}^{\phi\phi} - W_{nn}^{\phi\phi})} \right]. \tag{38}$$

■

After solving SOPF (35), feasible voltages are obtained by re-solving SOPF (35) with $\mathbf{r}$ fixed to the one retrieved from Proposition 9. In the next section, however, we assume that the set of complex power injections per node $n \in \mathcal{N}_+$ is a singleton and is fixed to the given load. Therefore, after solving (35) for $\mathbf{r}$, the procedure to obtain the corresponding voltages reduces to solving the load-flow problem. Recent results guarantee the uniqueness of voltage solutions in distribution networks [11], ridding us from re-solving (35).

V. Numerical tests

The standard IEEE 37-bus distribution feeder is adopted from [12]. Power and voltage bases are respectively $S_{\rm base} = 2500$ kVA and $V_{\rm base} = 4.8$ kV line-to-line. Network loads are assumed as constant-power wye. The total load amounts to $0.9828 + j0.4804$ pu comprising $0.3436 + j0.2194$ pu on phase a, $0.2682 + j0.1444$ pu on phase b, and $0.3709 + j0.1166$ pu on phase c. Series transformers are modeled as wye-g–wye-g. The network includes a slack bus at the substation, which is indexed to be node 1. We fix the voltage at the slack bus to $\mathbf{v}_1 = \{1, 1\angle -120^\circ, 1\angle 120^\circ\}$. The network contains an SVR located on edge $(2,3)$.

Bounds on voltages and turns ratios are set to $[v_{\min}, v_{\max}] = [0.9, 1.1]$ pu and $[r_{\min}, r_{\max}] = [0.9, 1.1]$. All computations are performed in MATLAB [13] and on a laptop computer with 8.0 GB RAM and 2 GHz CPU processor. The SDP (35) is solved by CVX [14]. MATLAB scripts for the ensuing tests

TABLE III
PERFORMANCE OF THE PROPOSED FORMULATION FOR OPTIMAL TAP-SELECTION OF SVRS

SVR	$\sum_{\phi\in\Omega} \mathrm{Re}[s_1^{\phi\,*}]$ (pu)	$\min \hat{\mathbf{v}}$ (pu)	$\max \hat{\mathbf{v}}$ (pu)	$\sum_{\phi\in\Omega} \mathrm{Re}[\hat{s}_1^{\phi}]$ (pu)	Opt. gap (%)
None	—	0.85	1.0000	1.0430	—
Wye	1.0358	0.92	1.05	1.0363	0.0544
Cl.-delta	1.0319	0.92	1.08	1.0355	0.3435
Op.-delta	1.0336	0.90	1.08	1.0351	0.1416

are provided online at the following link: http://github.com/hafezbazrafshan/MultiphaseVRs

For comparison purposes, using the Z-Bus method [11], a base voltage profile where the SVR block is replaced by its transmission line (equivalently, taps are set to 0) is computed for the IEEE 37-bus. The minimum and maximum voltage values as well as the power import thus obtained are listed in row 1 of Table III, respectively in columns 3–5. Problem (35) is then solved for a wye, closed-delta, and open-delta SVR on edge $(2,3)$. Its optimal value, denoted by $\sum_{\phi\in\Omega} \mathrm{Re}[s_1^{\phi\,*}]$ is reported in column 2 of Table III. By using the result of Proposition 9, the effective ratios for wye, closed-delta, and open-delta are respectively computed as $\mathbf{r}_{23} = \{0.9, 0.9, 0.9\}$, $\mathbf{r}_{23} = \{0.9313, 0.9125, 0.9125\}$, and $\mathbf{r}_{23} = \{0.9062, 0.9062\}$. It turns out that for all SVR types, the matrices of constraints (17e) and (17f) are almost rank-2 at the optimal solution of (35). The average ratio between the magnitude of the second largest eigenvalue to that of the dominant eigenvalue for matrices in (17e) is respectively 0.74, 0.73, and 0.61 for wye, closed-delta, and open-delta SVRs. The same ratio for (17f) is respectively 0.76, 0.73, and 0.56 for wye, closed-delta, and open-delta SVRs. The average ratio between the magnitude of the third largest eigenvalue to that of the dominant eigenvalue for all matrices in (17e) and (17f) is below 0.08.

Since matrices in (17g) and (17f) are not rank-1, and the formulation in (35) is a relaxation, the optimal value of (35) is a lower bound of the OPF (10). It is important to see how good this lower bound is. To this end, by fixing the SVR effective ratios to the computed ones, the Z-Bus load-flow is solved to obtain the nodal voltages using each SVR. The minimum and maximum values of the computed voltages $\hat{\mathbf{v}}$, are respectively reported in columns 3 and 4 of Table III. Since these values are within $[v_{\min}, v_{\max}]$, then the corresponding value of imported power, given by $\sum_{\phi\in\Omega} \hat{s}_1^{\phi}$ in column 5 of Table III, is an upper bound to the optimal solution of the original OPF (10). Notice that given $\hat{\mathbf{v}}$ and SVR ratios, the imported power per phase, $\hat{s}_1^{\phi}$, is easily calculated using (8). The corresponding optimality gap is computed as $100 \times \sum_{\phi\in\Omega} \mathrm{Re}\left[\hat{s}_1^{\phi} - s_1^{\phi}\right] / \mathrm{Re}[s_1^{\phi}]$ and is reported in column 6 of Table III.The optimality gap for all three cases is below 0.5%. The implication is that the solution of the proposed relaxed OPF in (35) provides reasonable taps for the SVRs. Voltage profiles and other network quantities can be obtained by visiting the github page.

VI. CONCLUSION, LIMITATIONS, AND FUTURE WORK

A general OPF framework for multi-phase distribution networks is presented that explicitly accounts for tap selection of various types of SVRs. Chordal SDP relaxation of power flow equations are leveraged to handle non-SVR edges. Novel linear relaxations are derived for the non-convex primary-to-secondary voltage relationship of SVR edges. The proposed problem is an SDP and can be solved efficiently. Preliminary results on a small distribution network verify that the method is successful at regulating nodal voltages while maintaining the power import of a distribution network within 1% of its optimal value. Despite these promising results, previous work has shown that SDP relaxation of equivalent OPF problems may or may not find the global solution of the problem [15]. Furthermore, the capability of modern SDP solvers in obtaining numerically accurate solutions of large-scale SDPs is still limited. Detailed investigations on the robustness of the proposed SDP formulation to various loading conditions and its scaling to larger networks are thus required. Such computational issues will be tackled in our future work.

REFERENCES

[1] W. H. Kersting, *Distribution System Modeling and Analysis*, 3rd ed. CRC Press, 2002.

[2] M. Bazrafshan and N. Gatsis, "Comprehensive Modeling of Three-Phase Distribution Systems via the Bus Admittance Matrix," *IEEE Trans. Power Syst.*, vol. 33, no. 2, pp. 2015–2029, Mar. 2018.

[3] E. Dall'Anese, Hao Zhu, and G. B. Giannakis, "Distributed Optimal Power Flow for Smart Microgrids," *IEEE Trans. Smart Grid*, vol. 4, no. 3, pp. 1464–1475, Sep. 2013.

[4] L. Gan and S. H. Low, "Convex relaxations and linear approximation for optimal power flow in multiphase radial networks," in *Proc. Power Systems Computation Conf.*, Wroclaw, Poland, Aug. 2014, pp. 1–9.

[5] ——, "Chordal relaxation of OPF for multiphase radial networks," in *Proc. Int. Symp. Circuits and Systems*, Melbourne, Australia, June 2014, pp. 1812–1815.

[6] A. S. Zamzam, N. D. Sidiropoulos, and E. Dall'Anese, "Beyond Relaxation and Newton-Raphson: Solving AC OPF for Multi-phase Systems with Renewables," *IEEE Trans. Smart Grid*, to be published. [Online]. Available: https://doi.org/10.1109/TSG.2016.2645220

[7] S. Paudyal, C. A. Canizares, and K. Bhattacharya, "Optimal Operation of Distribution Feeders in Smart Grids," *IEEE Trans. Ind. Electron.*, vol. 58, no. 10, pp. 4495–4503, Oct. 2011.

[8] B. A. Robbins, H. Zhu, and A. D. Dominguez-Garcia, "Optimal Tap Setting of Voltage Regulation Transformers in Unbalanced Distribution Systems," *IEEE Trans. Power Syst.*, vol. 31, no. 1, pp. 256–267, Jan. 2016.

[9] Y. Liu, J. Li, L. Wu, and T. Ortmeyer, "Chordal Relaxation Based ACOPF for Unbalanced Distribution Systems with DERs and Voltage Regulation Devices," *IEEE Trans. Power Syst.*, vol. 33, no. 1, pp. 970–984, Jan. 2018.

[10] T. H. Chen, M. S. Chen, T. Inoue, P. Kotas, and E. A. Chebli, "Three-phase cogenerator and transformer models for distribution system analysis," *IEEE Trans. Power Del.*, vol. 6, no. 4, pp. 1671–1681, Oct. 1991.

[11] M. Bazrafshan and N. Gatsis, "Convergence of the Z-Bus Method for Three-Phase Distribution Load-Flow with ZIP Loads," *IEEE Trans. Power Syst.*, vol. 33, no. 1, pp. 153–165, Jan. 2018.

[12] IEEE PES Distribution System Analysis Subcommittee's Distribution Test Feeder Working Group, "Distribution test feeders." [Online]. Available: http://ewh.ieee.org/soc/pes/dsacom/testfeeders/index.html

[13] MATLAB, *version R2016b*. The MathWorks Inc., 2010.

[14] M. Grant and S. Boyd, "CVX: Matlab software for disciplined convex programming, version 2.1," http://cvxr.com/cvx, Mar. 2014.

[15] D. K. Molzahn and I. A. Hiskens, "Convex Relaxations of Optimal Power Flow Problems: An Illustrative Example," *IEEE Trans. Circuits Syst. I: Reg. Papers*, vol. 63, no. 5, pp. 650–660, May 2016.